

INTERNATIONAL SOCIETY FOR SOIL MECHANICS AND GEOTECHNICAL ENGINEERING



This paper was downloaded from the Online Library of the International Society for Soil Mechanics and Geotechnical Engineering (ISSMGE). The library is available here:

<https://www.issmge.org/publications/online-library>

This is an open-access database that archives thousands of papers published under the Auspices of the ISSMGE and maintained by the Innovation and Development Committee of ISSMGE.

Consolidation Tests with Continuous Loading

Essais de Consolidation avec Chargement Continu

N. JANBU
O. TOKHEIM
K. SENNESET

Professor, Norwegian Inst. of Technology, Trondheim, Norway
Chief Geotechnical Engineer, Oslo Municipality, Norway
Chief Engineer, Norwegian Inst. of Technology, Trondheim, Norway

SYNOPSIS

Herein an exact solution is derived for oedometer consolidation under a variety of continuous loading procedures. This leads to simple formulas for interpretation of required deformation parameters and preconsolidation pressure.

A rapid test procedure has been introduced, simply called the CL-test (continuous loading). A tailor-made apparatus for CL-testing has been developed. A minicomputer controls the ratio between pore pressure and total pressure, in such a manner that this ratio can be kept at a maximum allowable level, for which the total testing time becomes minimum. Data acquisition, interpretation and plotting of results are computerized.

Typical results of CL-tests are presented and discussed in some detail. In addition, the results of several test series using different ratio of loading is presented and compared with more conventional test procedures. Particular emphasis is given to the determination of the preconsolidation pressure and deformation parameters.

INTRODUCTION

Continuous loading consolidation tests (CL) offer several advantages over conventional incremental load tests (IL). First of all the total time required for a CL-test is considerably reduced. Secondly, results can be presented directly as continuous stress-strain curves in arithmetic plots, which enable a straightforward interpretation. The smooth loading procedure is also favourable from the viewpoint of reduced sample disturbance.

Over the last decade a number of continuous loading procedures have been developed for oedometer testing, such as constant rate of strain (CRS), constant rate of loading and controlled gradient. Perhaps the CRS-test is so far the most well-known of the three.

In a pioneer test series Crawford (1964) used continuous loading in which the rate of loading was kept small enough to justify the neglect of the pore water pressure. Thus, the effective stress versus strain was readily obtained. Although Crawford registered the pore pressure in his samples, compressibility and permeability were not determined, presumably due to the lack of interpretation formulas.

Smith and Wahls (1969) developed approximate interpretation formulas for CRS-tests based on the observed pore water pressure at the imperious sample base, and an assumed pore pressure distribution throughout the sample. The pore pressure at the sample base was up to 50% of the applied total axial stress, thus permitting fast tests.

Lowe et al. (1969) introduced the controlled gradient consolidation test in which the rate of deformation is continuously adjusted to keep the base pore pressure constant. For such conditions very simple interpretation formulas were derived.

Wissa et al. (1971) elaborated further on the CRS-test, examining the transient period in which the base pore pressure is adjusting itself to imposed rate of deformation.

Aboshi et al. (1970) performed tests under constant rate of loading and derived the adequate interpretation formulas.

In order to optimize the continuous loading procedures it is necessary to abandon the restrictions imposed by either of the aforementioned procedures. Herein, it is shown that this can be achieved after deriving accurate solutions for the interpretation of the continuous consolidation problem, independent of the type of continuous loading procedure which is applied.

The influence of the rate of loading on the preconsolidation pressure is a question of vital importance in CL-testing. Early tests by Crawford (1964) revealed substantial increase in p_c' with increased rate of loading. Less significant effects were observed in a number of IL-tests by Senneset (1978), and in IL- and CL-tests by Ludvigsen (1978) and Senneset and Ludvigsen (1979).

The extensive work by Bjerrum (1967, 1972) on the nature of secondary consolidation and its

dependence of stress history, indicates that p_c should not be considered as a single value, but rather as a stress range over which the rate of secondary consolidation gradually increases. The reasons behind this observation will be discussed in view of the results obtained herein.

THE NEW EQUIPMENT

A rational use of the advantages of continuous loading procedures requires such sophisticated equipment as a logging devices, a computer, transducers, and plotting units.

Fig. 1 is a general view of our new oedometer equipment for CL-testing. The oedometer sample is of standard size (area 20 cm², height 2 cm) and is confined by a steel ring and a porous, sintered bronze disc at the top. The base is impervious, but contains a small porous filter-stone with a pore pressure transducer beneath it. The oedometer is placed in a rig containing an electromechanical press and transducers to record vertical load, displacement and pore pressure.

The photo also give the layout of the control unit box. This unit can monitor the following recordings: Deformation of sample, load, pore pressure and rate of deformation, all in engineering units. The control unit is equipped for direct connection to a Hewlett Packard minicomputer (HP 1000). The computer has the ability to do measurements over a wide range, to scale and linearize signals and to store the data in specified data files. The datafiles may be processed during or after the test to produce test result diagrams on the x-y plotter (or at a screen), and arrange test result tables on the printer, without affecting the high priority programs running towards ongoing tests for process control and data acquisition.

A brief description of the oedometer equipment with some specifications is given below:

- The press unit and the rig are designed for samples with different size.
- The DC-motor and the gear allow a range in vertical movement from 0.0022 mm/min to 0.18 mm/min.
- The LVDT-transducer for measurement of deformation has a capacity of ± 5 mm. The transducer for pore pressure has a measuring range of 0-103 kPa. The force transducer is easy to shift to keep a proper measuring range suited for the type of soil. Max. load capacity is 20 kN. The present transducer has a range of 0 - 2.5 kN.
- The control unit scale and monitor the measured values in engineering units, and is able to stop the test when preset limitations are reached (max. load or max deformation).
- The (false) deformations is the rig and other parts of the oedometer, is corrected for in the computer program.

The computer carries out all interpretations of the tests and produces the required diagrams.

THEORY FOR CL-TEST INTERPRETATION

It will be shown herein that a single set of formulas can be used for interpretation of all the available CL-test procedures. Thus, this set of formulas represent a general synthesis of all CL-procedures. Hence the specific restrictions imposed by each separate procedure are overcome.

During CL-tests the following data are recorded continuously, see Fig. 2.

- q = applied load (vertical)
- δ = sample compression
- u_p = pore pressure at impervious base.

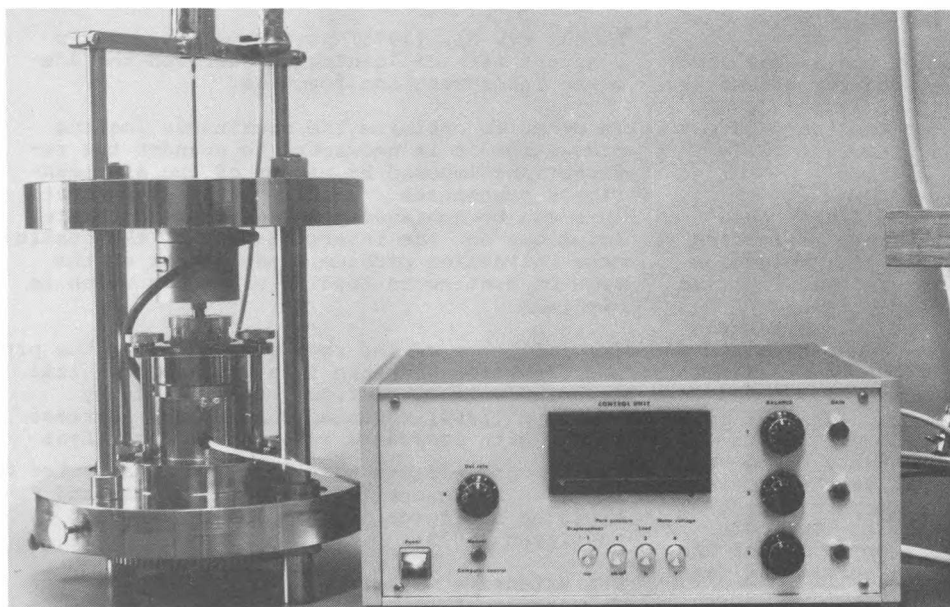


Fig. 1.

A new oedometer for continuous loading.

Hence, the time derivatives of these quantities are also known, and stored in the data acquisition system. These derivatives are denoted \dot{q} , $\dot{\delta}$ and \dot{u}_b , respectively.

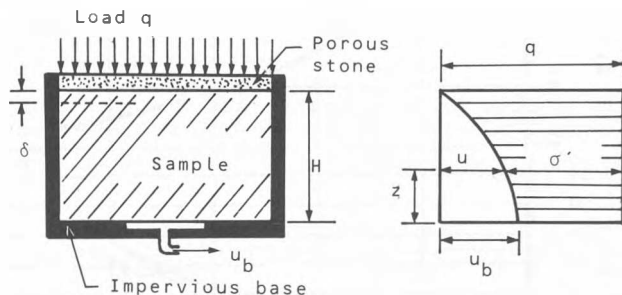


Fig. 2. CL-test. Principle and notations.

When these data are known, one can use the defining equations for tangent modulus (M), permeability (k) and coefficient of consolidation (c_v) to arrive at the following interpretation formula (see Appendix):

$$M = \alpha_M \frac{\dot{q}H}{\dot{\delta}} \quad (1)$$

$$k = \alpha_k \frac{\gamma_w H \dot{\delta}}{2\dot{u}_b} \quad (2)$$

$$c_v = \alpha_c \frac{\dot{q}H^2}{2\dot{u}_b} \quad (3)$$

wherein H = initial sample height, and $\gamma_w = g\rho_w$ = unit weight of water.

The dimensionless α -coefficients are all functions of the ratio between \dot{u}_b and \dot{q} , denoted λ

$$\lambda = \frac{\dot{u}_b}{\dot{q}} = \frac{du_b}{dq} \quad (4)$$

This pore pressure-load ratio (PLL-ratio) will always range between 0 and 1.0. In an oedometer the condition $\lambda = 0$ covers a fully drained condition, either due to sufficiently slow loading or sufficiently high permeability, while $\lambda = 1$ for a fully undrained and no volume-change condition. The secret of successful CL-tests, and the potentiality for reaching optimal efficiency and economy with CL-tests, is to be found in understanding the role of λ in the subsequent theory.

To arrive at the α -coefficients, it is necessary to obtain the pore pressure distribution over the sample height, Fig. 2. In the Appendix it is shown that for $\lambda = \text{constant}$ during a CL-test (or portion of it) a rigorous solution of the differential equation leads to the following pore pressure distribution, in dimensionless terms, when

$$f(\xi, \lambda) = u/u_b$$

$$f(\xi, \lambda) = \frac{\cosh a - \cosh a \xi}{\cosh a - 1} \quad (5)$$

where

$$(1-\lambda) \cosh a = 1 \quad (6)$$

This numerical solution is illustrated in Fig. 3. One should note that $\lambda = 0$ for $a = 0$ and $\lambda = 1$

for $a = \infty$. Moreover, one finds that

$$\lim_{\lambda \rightarrow 0} f(\xi, \lambda) = 1 - \xi^2 \quad (5a)$$

$$\lim_{\lambda \rightarrow 1} f(\xi, \lambda) = 1, \text{ except for } \xi = 1 \quad (5b)$$

This means that the second degree parabola is a rigorous solution for $\lambda = 0$, as has already been known for some time. The approximate solution obtained by Tokheim and Janbu (1976) is fully covered by the following pore pressure function

$$f(\xi, \lambda) = 1 - \xi^n \quad (7)$$

$$n = \frac{4(3 - 2\lambda)}{6 - 5\lambda} \quad (8)$$

It is seen that $n = 2$ for $\lambda = 0$ exact while $n = 4$ for $\lambda = 1$. The limiting parabola ($n = 4$) for $\lambda = 1$ is dotted in Fig. 3. for comparison.

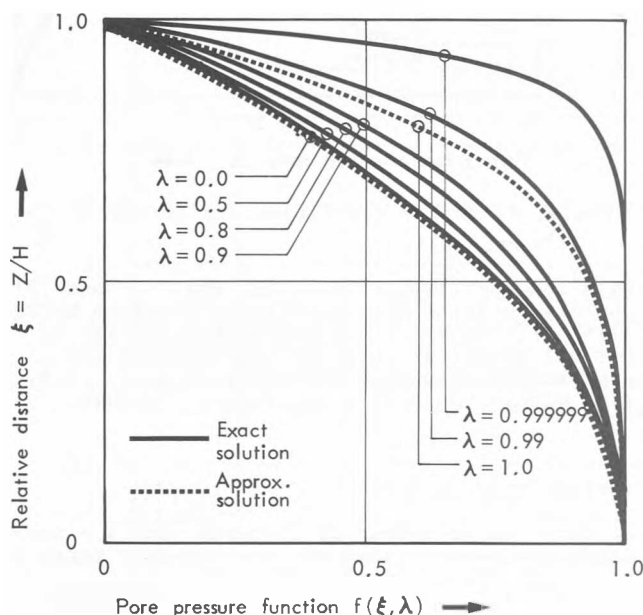


Fig. 3. Distribution of excess pore pressure across sample. Exact and approximate value.

With $f(\xi, \lambda)$ known one can obtain the interpretation coefficients α as follows, see Appendix

$$\alpha_M = 1 - \lambda \int_0^1 f(\xi, \lambda) d\xi \quad (9)$$

$$\alpha_k = -2/f'(1, \lambda) \quad (10)$$

$$\alpha_c = \alpha_M \alpha_k \quad (11)$$

Using the exact solution, Eqs. (5) and (6), one gets

$$\alpha_M = \frac{\tanh a}{a} \quad (12)$$

$$\alpha_k = \frac{2(\cosh a - 1)}{a \sinh a} \quad (13)$$

$$\alpha_c = \frac{2(\cosh a - 1)}{a^2 \cosh a} \quad (14)$$

Using the established formula $(1 - \lambda) \cosh a = 1$

all α -coefficients are calculated as functions of λ , and the result is shown in Fig. 3.

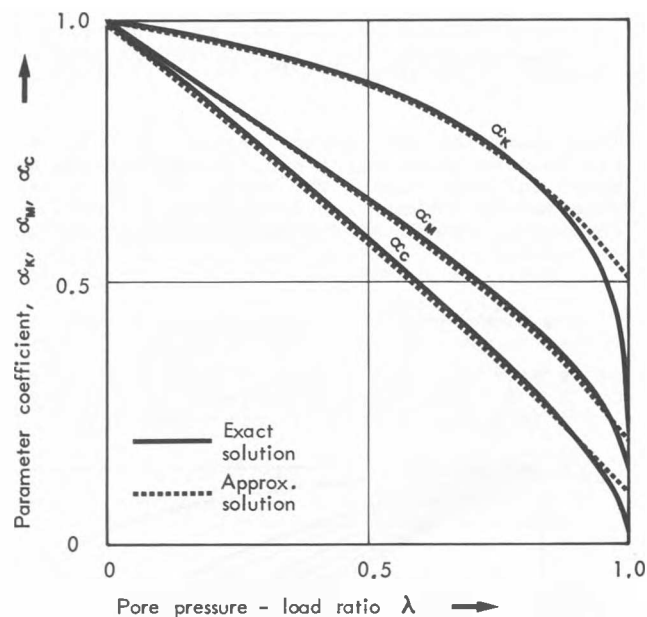


Fig. 4. Parameter coefficients α versus PPL-ratio, λ .

With the approximate solution, Eqs. (7) and (8), one also obtains the approximate α -values by Eqs. (9)-(11). These values are dotted in Fig. 4. For all practical purposes the rigorous and approximate solutions are equal up to $\lambda \sim 0.8$, i.e. within the entire applicable λ -range.

TYPICAL TEST RESULTS

So far a large number of CL-tests with $\lambda = \text{constant}$ has been carried out on different types of clay, see eg. Ludvigsen (1978).

The most recent CL-test series were performed on Risvöllan Clay, which is characterized in broad terms by the following data:

$w = 39-49\%$ (45%)	$w_L - w_p = 12\% \pm$
$\% < 2\mu = 45-55\%$ (49%)	$s_u = 40 \text{ kPa} \pm$
$\gamma = 18 \text{ kN/m}^3$	Sensitivity = $10 \pm$

where the average values are given in parenthesis. It is an overconsolidated clay with a relatively large scatter in water content and undrained strength, and it is layered.

For $\lambda = 0.3$ the computer results of two CL-tests are contained in Fig. 5, in which ϵ , M , c_v , and δ are all shown versus effective vertical stress σ' or p' . The following trend is quite clear: The preconsolidation pressure p_c' is well identified in all four diagrams to be about 250 kPa, as compared to the present overburden of $p_0' = 105 \text{ kPa}$. Moreover, the gradually increasing structural breakdown between p_0' and p_c' is remarkably clear in both resistance plots, $M-\sigma'$ and $c_v-\sigma'$. It is also very interesting to note the pro-

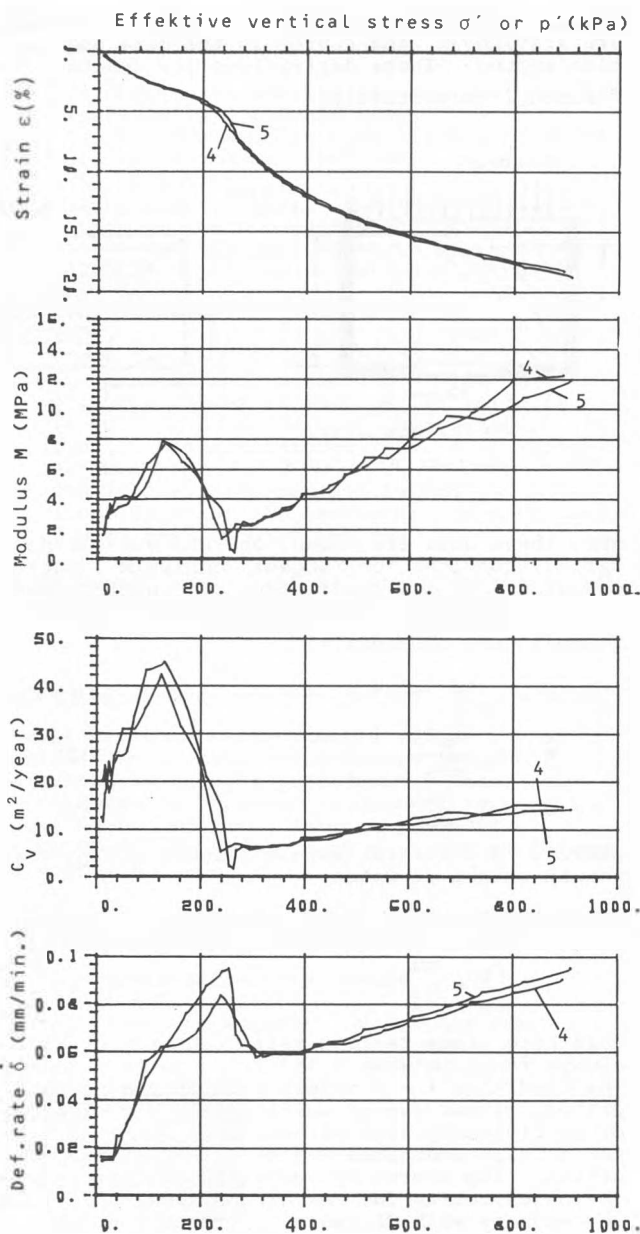


Fig. 5. Test results of CL-test No. 4 and 5 on Risvöllan Clay with $\lambda=0.3$.

nounced changes in deformation rate δ required to keep $\lambda = 0.3 = \text{constant}$.

The results of all 12 tests on Risvöllan Clay are plotted together in Fig. 6. The λ -value varied between 0.2 and 0.5, and for each λ three tests were conducted. It is almost surprising to observe the small scatter in ϵ , M and c_v considering the large variation in applied λ and the substantial differences in water content between the individual samples.

Fig. 7 contains a comparison between two CRS-tests on Risvöllan Clay, where the two speeds applied are 0.6% versus 6% per hour. Broadly

speaking the M and c_v variations are not affected by the speed, and apparently the largest speed is easier to handle and of course quicker and less expensive. Even at 6% per hour the excess pore pressure is small ($\lambda < 0.1$).

FACTORS OF INFLUENCE

Each test has been interpreted for modulus numbers (m) and preconsolidation pressures (p_c') and these vital data are plotted versus the pore

pressure ratios λ in Figs. 8 and 9.

Fig. 8 contains the 12 CL-results from the Risvöllan Clay together with two CRS-tests at $\dot{\epsilon} = 0.6$, and 6% per hour. It is seen that m tends to decrease with increasing λ while p_c' appears to increase slightly with increasing λ . As far as the absolute value of M is concerned these are two compensating effects (the one kills the other). For the two CRS-tests the tendency is seemingly reversed.

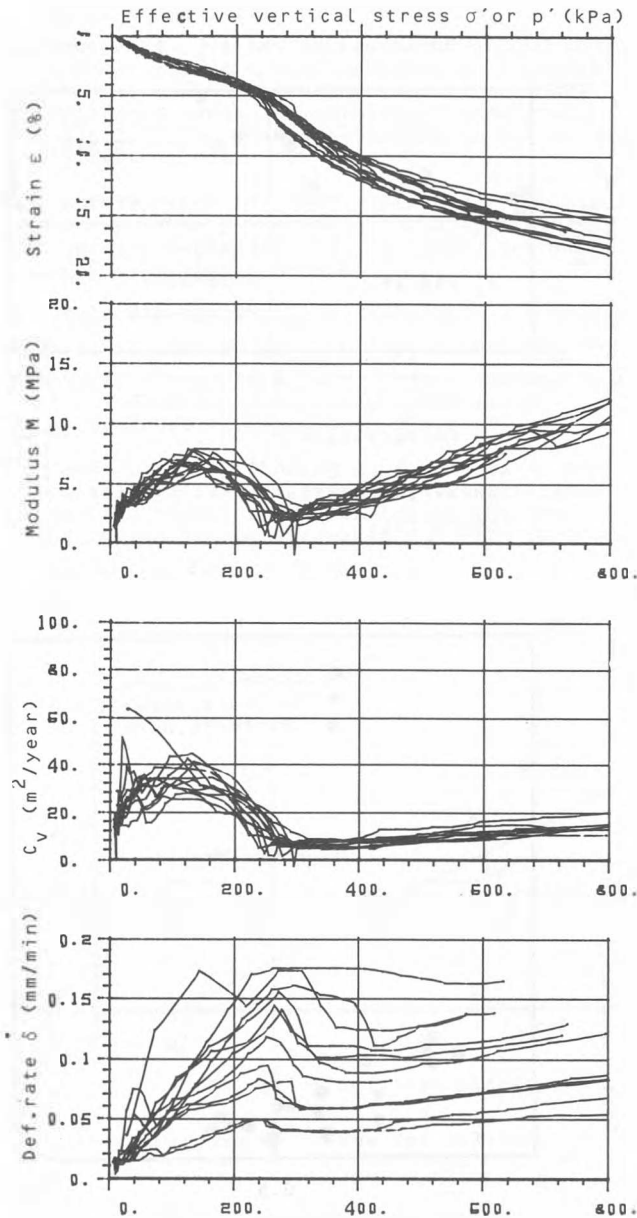


Fig.6. Test results of 12 CL-tests on Risvöllan Clay with λ =constant Range $\lambda=0.20-0.50$.

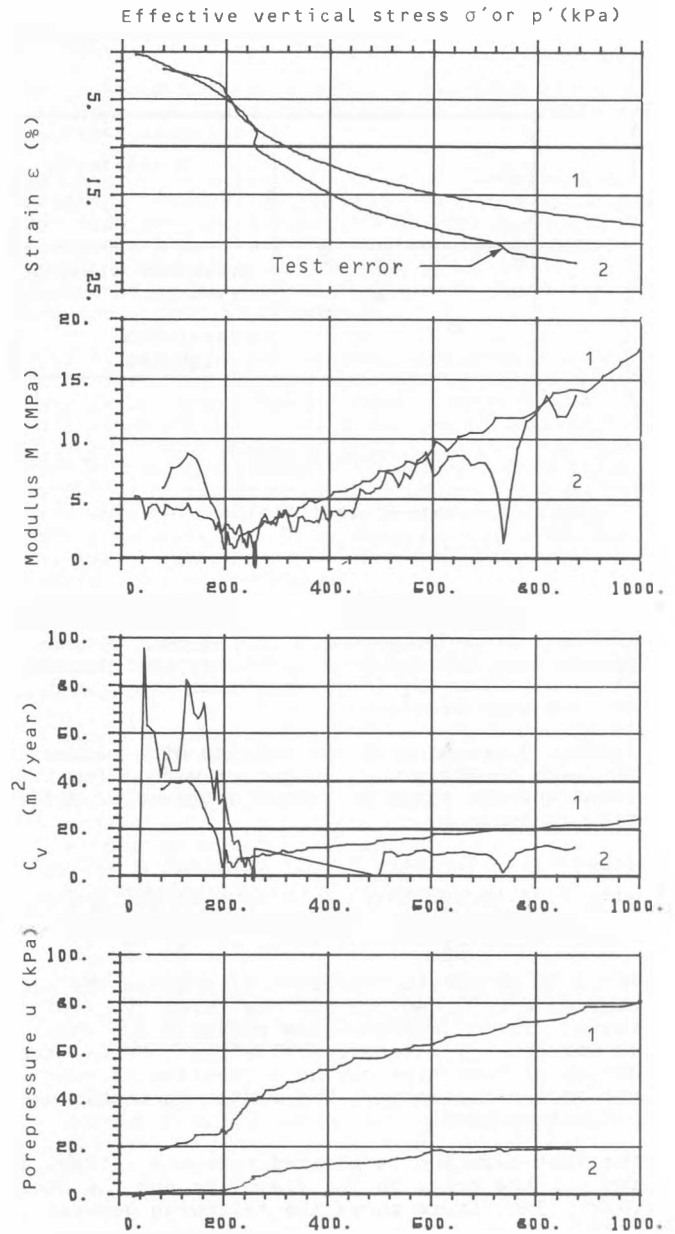


Fig.7. Test results of 2 CRS-tests on Risvöllan Clay with $\dot{\epsilon}=6.0\%$ pr. hour (1) and 0.6% pr. hour (2).

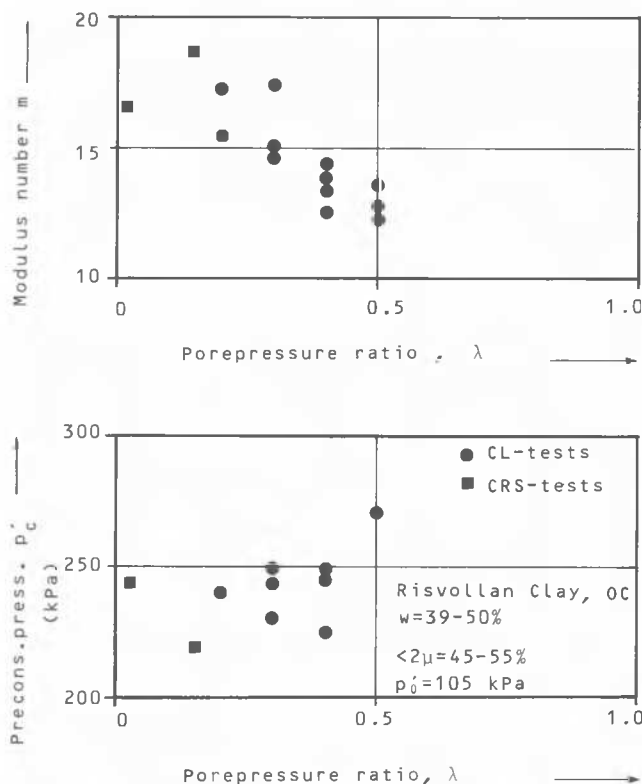


Fig.8. Summary of test results for the Risvollan Clay.

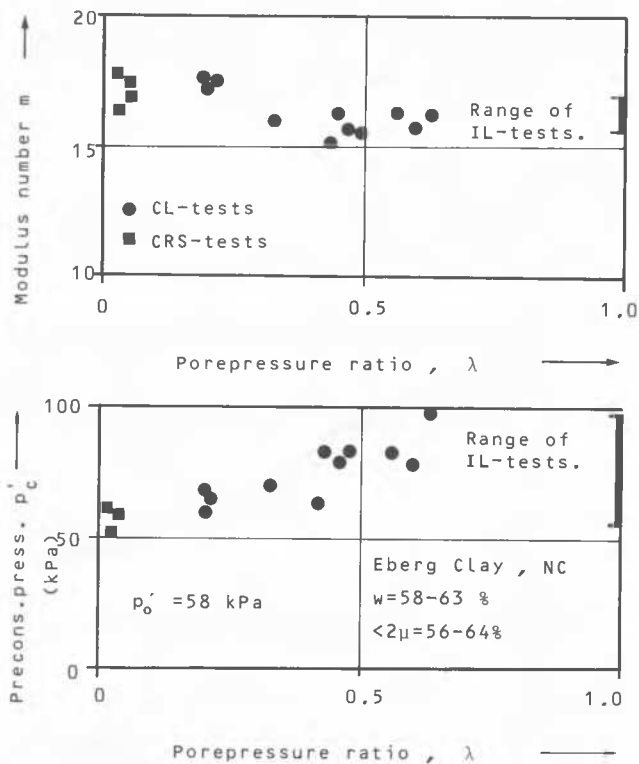


Fig.9. Summary of test results for the Eberg Clay.

It is of particular interest to note that even the rate of deformation of 6% per hour corresponds to a low value of $\lambda < 0.15$, even though it is a relatively fat, impervious clay, with ca. 50% clay fraction.

In Fig. 9 are plotted the results of a series of CL-tests on Eberg Clay, together with a few CRS-tests and the range of values obtained by different IL-tests.

This figure indicates almost constant m and p_c' with λ , although there is a very slight indication of a similar trend as in Fig. 8. The clay is almost normally consolidated, i.e. $p_c' \sim p_0'$.

It is of particular interest to observe the close coherence obtained for all the three types of tests. The differences are actually too small to warrant any relative evaluation. Hence, the choice of test type may be a question of convenience and economy. The latter is highly dependent on time.

The test duration is plotted versus λ in Fig. 10 for all the tests on the Risvollan and the Eberg clay. The figure shows the following general trend:

In the overconsolidated Risvollan clay the testing time is roughly half of that of the normally consolidated Eberg clay, and for $\lambda = 0.35-0.60$, the full testing time is less than 1 hour for

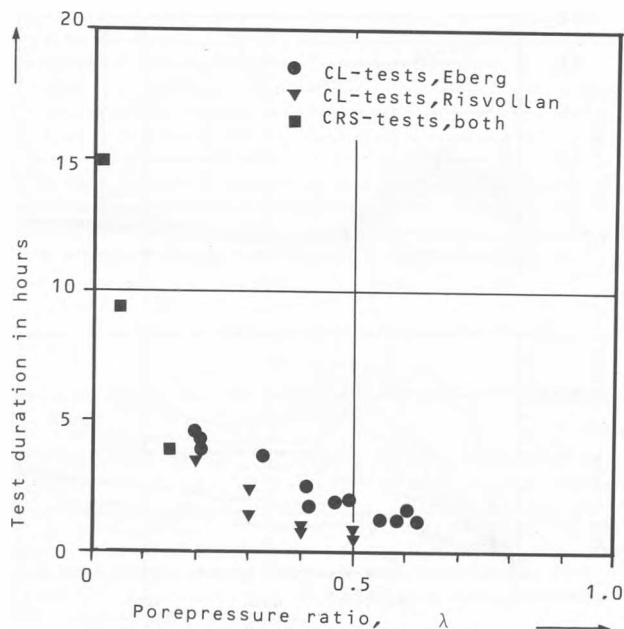


Fig.10. Summary of test duration as function of λ .

the OC-clay, and less than 2½ hours for the NC-clay. In contrast, the CRS-tests lasted from 9 to 40 hours. It should be noted, however, that in our opinion the tendency today is to use much too slow deformation rates in the tentative standards of CRS-tests. In most clays a rate of 5% to 10% per hour should be acceptable. An exception may be the high-plastic clays with $w \geq 100\%$ in which case one may have to use about 1% to 2% per hour.

Fig. 11 is an idealized $M-\sigma'$ curve for intact OC-clays, based on the statistical average of Fig. 6: During reloading in an oedometer M increases up to in situ overburden p_0' , whereafter it stays fairly constant (at M_{OC}). Then it decreases, due to structural breakdown which continues until the preconsolidation pressure p_c' is reached. Thereafter, in the normally consolidated range, M increases linearly with σ' , and it often points backwards to p_0' as the new virgin origin.

The stress range $\Delta\sigma'$ over which the structural breakdown takes place varies with type of soil and testing procedure. It is a very important field for further research.

The value of $M_{OC} = m_{OC} (p_0' + a)$ where a = attraction (20 to 50% of $\Delta p_c' = p_c' - p_0'$) reflects the residual, isotropic in situ stress induced by $\Delta p_c'$. The value of m_{OC} lies often in the range of 30-60 for Norwegian clays.

The most pleasant finding so far seems to be how little p_c' is influenced by variations in CL-testing techniques, even though the general trend appears to be increased p_c' with increased $\dot{\epsilon}$, especially for $\lambda > 0.35$.

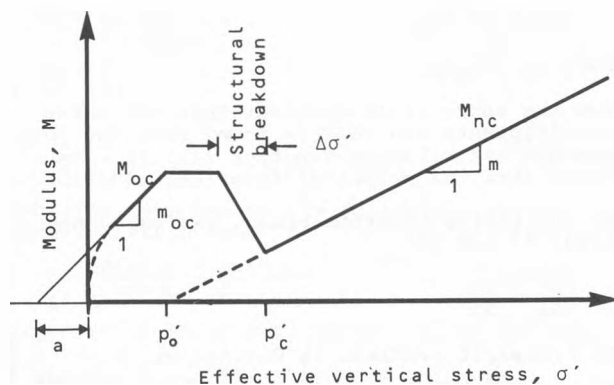


Fig.11. Idealized $M-\sigma'$ curve for OC-clay.

SUMMARY

Over the last 10 years CL-testing of different types is slowly being implemented in various parts of the world. Considering the large potential gains at stake, it is surprising that the use of CL-testing is progressing so slowly both in practice and in research. Perhaps the most important reasons are:

- uncertainties about the reliability of the various available test procedures
- unknown background for test interpretations
- lack of sufficiently advanced equipment and data logging systems.

It is hoped that this article may help removing the apparent obstacles against a more widespread use of CL testing.

In this article the principle of CL-testing is briefly reviewed, and a relatively new apparatus for such testing is described. The apparatus is highly automatized, and the interpretation is computerized so that the test results can be presented in report-ready diagrams immediately after the test is completed.

This development was rapidly advanced after Tokheim (1976) derived an accurate solution for the CL-process for constant ratio between base pore pressure and total load, herein called λ . This solution, together with initial tests disclosed that the deformation parameters obtained were nearly independent of λ below say 0.8. This finding indicated that the testing time for Norwegian clays could be reduced substantially, say from 5 hours to less than one hour, with little loss of accuracy.

Based on the results of several series of CL-tests on intact clays the following observations are made (all diagrams referred to are arithmetic plots):

- For one tube sample 12 tests with $\lambda = \text{constant}$ ($=0.2-0.3-0.4$ and 0.5) were carried out and all tests were plotted in the same diagrams. These condensed plots showed a surprising consistency in parameter variations with effective stress, independent of λ .
- A comparison between CRS-tests of widely different strain rate (0.6% versus 6% per hour) indicate that the differences between the obtained deformation parameters are so small, (and unsystematic) that the very low-speed CRS-tests may be just a waste of time. It may at least be very difficult to find a logic defense for it.
- The preconsolidation pressure may be deducted from one or all of the following arithmetic plots: $\epsilon-\sigma'$, $M-\sigma'$, $c_v-\sigma'$ and $\delta-\sigma'$, when $\lambda=\text{constant}$.

- For an overconsolidated clay (Risvöllan) the modulus versus effective stress curve shows the following general trend (Fig. 11): M increases up to M_{OC} at p'_0 with a negative σ' -intercept (equals attraction, a). Then M_{OC} stays fairly constant over ca. $\frac{1}{2}\Delta p'_C = \frac{1}{2}(p'_C - p'_0)$, whereafter M rapidly decreases towards p'_C due to structural breakdown. After p'_C an almost linear increase in $M = m(\sigma' - p'_0)$ is observed (with a positive stress intercept $\sim p'_0$).
- The parameter c_v versus σ' varies in a manner similar to $M - \sigma'$ (because $c_v = Mk/\gamma_w$, and k is much less affected by σ' and p'_C than M).
- The diagram $\delta - \sigma'$ shows the following trend (Fig. 6): δ increases almost linearly with σ' up to p'_C after which δ stays fairly constant. Hence, the preconsolidation pressure can easily be determined.
- Even in CRS-tests (where λ varies, but is often below 0.1) the $u - \sigma'$ plot indicate a change in variation around p'_C (see Fig. 7).
- The magnitude of p'_C appears to be the same both for CL- and CRS-testing if $\lambda \leq 0.35$. However, when λ is increased very much beyond this value (say to 0.6) p'_C tends to increase slowly.
- The magnitude of m is also unaffected by variations in $\lambda < 0.3$, while m may decrease slightly with increasing $\lambda > 0.35$.

In conclusion, it is our considered opinion that CL-testing is to be preferred to IL-testing for several reasons, but mainly for quality and reliability of test results, and for expedience and economy.

ACKNOWLEDGEMENT

The authors acknowledge with gratitude the valuable contribution by Eng. A. Selnæs in programming the CL-test procedures all the way to plotting report-ready test result diagrams. Much credit is also due to Lab.ass. A. Jensen for carrying out the laboratory tests, and to Civ.Eng. A. Stordal for extensive help in preparation of test data and figures.

APPENDIX: DERIVATIONS

Let the pore pressure distribution across the sample be given by a function f so that

$$u = fu_b \quad (A-1)$$

The average f -value (\bar{f}) then becomes

$$\bar{f} = \int_0^1 f d\xi \quad (A-2)$$

where $\xi = z/H$, see Fig. 1.

Hence the average effective stress across the sample is

$$\bar{\sigma}' = q - \bar{f}u_b \quad (A-3)$$

By definition, the tangent modulus is

$$M = \frac{d\bar{\sigma}'}{d\epsilon} = \frac{d(q - \bar{f}u_b)}{d(\delta/H)} = (1 - \lambda\bar{f})H \frac{dq}{d\delta}$$

abbreviated to the form

$$M = \alpha_M H \frac{dq}{d\delta} = \alpha_M \frac{\dot{q}H}{\dot{\delta}} \quad (A-4)$$

Wherein $\alpha_M = 1 - \lambda\bar{f}$ (A-5)

$$\text{and } \lambda = \frac{du_b}{dq} = \frac{\dot{u}_b}{\dot{q}} \quad (A-6)$$

By definition, the permeability k is defined by the Darcy equation $v = ki$. At the pervious boundary $v = \dot{\delta}$ and $i = -du/d(\gamma_w z)$ for $\xi = 1$, hence

$$k = - \frac{\gamma_w H \dot{\delta}}{u_b f'(1)} = \alpha_K \frac{\gamma_w H \dot{\delta}}{2u_b} \quad (A-7)$$

where $\alpha_K = -2/f'(1)$ (A-8)

wherein $f'(1)$ equals $df/d\xi$ for $\xi = 1$.

From classical consolidation theory $c_v = Mk/\gamma_w$.

When utilizing Eqs. (A-4) and (A-7) one gets

$$c_v = \alpha_C \frac{\dot{q}H^2}{2u_b} \quad (A-9)$$

where $\alpha_C = \alpha_M \alpha_K$ (A-10)

From the above it is apparent that the three α -coefficients are readily found when the pore pressure distribution function $f(\xi)$ is established from the proper differential equation.

The continuity equation reads, see eg. Janbu (1965, 67 and 69).

$$\frac{\partial v}{\partial z} = \frac{\partial \epsilon}{\partial t} \quad (A-11)$$

The hydraulic gradient is defined as $i = -\frac{1}{\gamma_w} \frac{\partial u}{\partial z}$ which gives the Darcy velocity

$$v = - \frac{k}{\gamma_w} \frac{\partial u}{\partial z} \quad (A-12)$$

Reformulating $\frac{\partial \epsilon}{\partial t} = \frac{\partial \epsilon}{\partial \sigma'} \frac{\partial \sigma'}{\partial t}$

and observing that, by definitions,

$$M = \frac{\partial \sigma'}{\partial \epsilon} = \frac{d\sigma'}{d\epsilon}, \text{ and } \frac{\partial \sigma'}{\partial t} = \frac{\partial}{\partial t} (q - u)' = \dot{q} - \frac{\partial u}{\partial t}$$

one finds $\frac{\partial \epsilon}{\partial t} = \frac{1}{M} (\dot{q} - \frac{\partial u}{\partial t})$ (A-13)

Eqs. (A-11) to (A-13) yields

$$\frac{\partial}{\partial z} \left[\frac{k}{\gamma_w} \frac{\partial u}{\partial z} \right] = \frac{1}{M} \left[\frac{\partial u}{\partial t} - \dot{q} \right] \quad (A-14)$$

For k being independent of z and using the classical abbreviation

$$c_v = \frac{Mk}{\gamma_w} \quad (A-15)$$

the differential equation is reduced to

$$c_v \frac{\partial^2 u}{\partial z^2} = \frac{\partial u}{\partial t} - \dot{q} \quad (A-16)$$

When using the dimensionless variables

$$\xi = z/H \quad T = \frac{tc_v}{H^2} \quad (A-17)$$

one gets $\frac{\partial^2 u}{\partial \xi^2} = \frac{\partial u}{\partial T} - \frac{\dot{q}H^2}{c_v}$ (A-18)

Introducing $u = fu_b$, $f = f(\xi, \lambda)$ (A-19)

where $\lambda = \frac{\dot{q}H^2}{c_v} = \frac{du_b}{dq}$ (A-20)

the differential equation (A-18) is further reduced to the following, for $\lambda = \text{constant}$,

$$f'' - \frac{2}{\alpha_c} (\lambda f - 1) = 0 \quad (A-21)$$

where $f'' = \partial^2 f / \partial \xi^2$, and α_c is defined by Eq. (A-9)

Substituting $F = \lambda f - 1$, $2\lambda = a^2 \alpha_c$ (A-22)

Eq. (A-21) is transferred to $F'' - a^2 F = 0$

with the solution $F = C_1 \sinh a\xi + C_2 \cosh a\xi$

Hence $f = \frac{1}{\lambda} [1 + C_1 \sinh a\xi + C_2 \cosh a\xi]$ (A-23)

With the boundary conditions

$$\begin{aligned} f &= 0 & \text{for } \xi &= 1 \\ f' &= 0 & \text{for } \xi &= 0 \\ f &= 1 & \text{for } \xi &= 0 \end{aligned} \quad (A-24)$$

one obtains

$$\begin{aligned} C_1 &= 0, \quad C_2 \cosh a = -1, \\ (1 - \lambda) \cosh a &= 1 \end{aligned} \quad (A-25)$$

which finally leads to the following pore pressure distribution

$$f = \frac{\cosh a - \cosh a\xi}{\cosh a - 1} \quad (A-26)$$

wherein $(1 - \lambda) \cosh a = 1$, hence $f = f(\xi, \lambda)$, Fig. 3

The average \bar{f} and $f'(1)$ are now obtained

$$\bar{f} = \frac{a \cosh a - \sinh a}{a \cosh a - a}$$

$$f'(1) = - \frac{a \sinh a}{\cosh a - 1}$$

This average \bar{f} as function of λ is shown in Fig. 12.

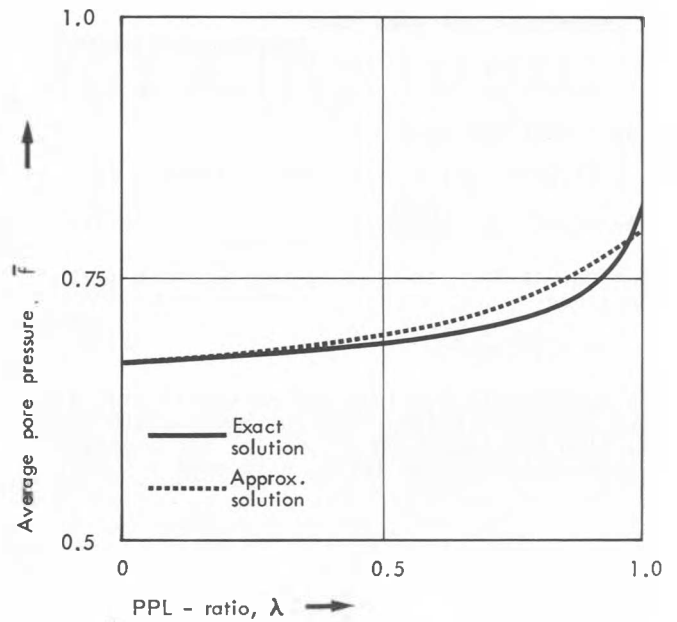


Fig. 12 Average pore pressure coefficients versus PPL-ratio, λ .

Using Eqs. (A-5), (A-8) and (A-10) together with (A-26) one gets

$$\begin{aligned} \alpha_M &= \frac{\tanh a}{a}, \quad \alpha_k = \frac{2(\cosh a - 1)}{a \sinh a}, \\ \alpha_c &= \frac{2(\cosh a - 1)}{a^2 \cosh a} \end{aligned} \quad (A-27)$$

All α -values are now obtained as function of λ only by $(1 - \lambda) \cosh a = 1$, Fig. 4.

In early 1970's our institute at NTH utilized an approximate f -function of the parabolic form.

$$f = 1 - \xi^n \quad (A-28)$$

with n -values between 2 and 4.

Using Eqs. (A-5), (A-8) and (A-10) one finds very easily

$$\begin{aligned} \alpha_M &= 1 - \frac{n}{1+n} \lambda, \quad \alpha_k = \frac{2}{n}, \\ \alpha_c &= \frac{2}{n} (1 - \frac{n\lambda}{1+n}) \end{aligned} \quad (A-29)$$

In 1975-76 Tokheim obtained an approximate, boundary - correct solution by integrating the differential equation (A-16) twice for an assumed initial f -function (for $n = 2$) and assuming

$\lambda = \text{const}$. This approximate solution read

$$f = (1 - \xi^2) (1 + C\xi^2), \quad (A-30)$$

where $C = \frac{\lambda}{6-5\lambda}$

By inspection one sees that

$$\lambda = 0 \text{ for } C = 0, \text{ i.e. } f = 1 - \xi^2, \text{ or } n = 2$$

$$\lambda = 1 \text{ for } C = 1, \text{ i.e. } f = 1 - \xi^4, \text{ or } n = 4$$

From (A-30) one gets

$$f'(1) = -2(1 + C) = -2(6 - 4\lambda)/(6 - 5\lambda)$$

$$\text{leading to } \alpha_k = \frac{6-5\lambda}{6-4\lambda} \quad (\text{A-31})$$

from Eq. (A-8). Equalizing this α_k with (A-29) one finds

$$n = \frac{4(3 - 2\lambda)}{6 - 5\lambda} \quad (\text{A-32})$$

The approximate α -values are dotted in Fig. 4, from which it is seen that the approximate solution has been good enough for all practical purposes, because so far we have used $\lambda < 0.7$.

REFERENCES

- Aboshi, H. Yoshikumi, H & Maruyama, S. (1970). Constant loading rate consolidation test. *Soils and Foundations*, (10), 1, 43-56.
- Bjerrum, L. (1976). Engineering geology of normally - consolidated marine clays as related to the settlements of buildings. Seventh Rankine Lecture. *Géotechnique* (17), 2, 83-118.
- Bjerrum, L. (1972). Embankments on soft ground. State of the art report. *Proc. ASCE Spec. Conf.*, (2), 1-54, Purdue.
- Bjerrum, L. (1972). The effect of rate of loading on the p_c - value observed in consolidation tests on soft clays. Discussion. *Proc. ASCE Spec. Conf.*, Purdue.
- Crawford, CB. (1964). Interpretation of the consolidation test. *Proc. ASCE*, (90), SM5, 87-102.
- Janbu, N. (1963). Soil compressibility as determined by oedometer and triaxial tests. *Proc. ECSMFE*, (1), 19-25, Wiesbaden.
- Janbu, N. (1965). Consolidation of clay layers based on nonlinear stress-strain. *Proc. 6. ICSMFE*, (1) 83-87, Montreal.
- Janbu, N. (1967). Settlement calculations based on the tangent modulus concept. (Moscow-lectures). *Bulletin 2*, SM, Norw. Inst. of Techn., 1-57, Trondheim.
- Janbu, N. (1969). The resistance concept applied to deformations of soils. *Proc. 7. ICSMFE*, (1) 191-196, Mexico.
- Lowe, J III, Jonas, E. & Obrician, V. (1969). Controlled gradient consolidation test. *Proc. ASCE*, (95), SM1, 77-97.
- Nowacki, E.H.H. (1973). Onedimensional consolidation with stress- and time dependent material properties. (In Norwegian). Dr. ing. Thesis, SM, Norw. Inst. of Techn. 1-168, Trondheim.
- Ludvigsen, N. (1978). Consolidation test procedures. Comparisons. Diploma thesis (in Norwegian), Div. SMFE, the Norw. Inst. of Techn., Trondheim.
- Selnæs, A. (1979). CL-oedometer. Equipment description. (In Norwegian). Internal Report, SM, Norw. Inst. of Techn., 39 pages, Trondheim.
- Senneset, K. (1973). Oedometer procedures. (In Norwegian). Internal Report SM, Norw. Inst. of Techn., Trondheim.
- Senneset, K. and Ludvigsen, N. (1979). Settlement parameters determined by CL-tests. (In Norwegian) *Proc. NGM-79*, (1) 620-631, Esbo, Finland.
- Sällfors, G. (1975). Preconsolidation pressure of soft, high-plastic clays. Dr. Thesis, Chalmers, Gothenburg.
- Smith, R.E. & Wahls, H.E. (1969). Consolidation under constant rates of strain. *Proc. ASCE*, (95), SM2, 519-539.
- Terzaghi, K. (1923). Die Berechnung der Durchlässigkeit des Tones aus dem Verlauf der Hydrodynamischen Spannungsercheinungen. *Sitzungsberichte. Mathematisch - naturwissenschaftliche Klasse*, Part 2a, (132), 3/4, 125-138, Akademie der Wissenschaften, Vienna.
- Tokheim, O. & Janbu, N. (1976). A continuous consolidation test. Internal Report, SM, Norw. Inst. of Techn., Trondheim.
- Wissa, A.E.Z., Christian, J.T., Davis, E.H. & Heiberg, S. (1971). Consolidation at constant rate of strain. *Proc. ASCE*, (97), SM10, 1393-1413.